IJE TRANSACTIONS B: Applications. Vol. 28, No. 11, (November 2015) 1671-1679

International Journal of Engineering

Journal Homepage: www.ije.ir

# Liquid Sloshing Effect Analysis on Lateral Dynamics of an Articulated Vehicle Carrying Liquid for Various Filled Volumes

M. A. Saeedi*, R. Kazemi, S. Azadi

*Department of Mechanical Engineering, K. N. Toosi University of Technology, Tehran, Iran.*

*PAPER INFO*

*Paper history:*
Received 15 July 2015
Received in revised form 12 November 2015
Accepted 19 November 2015

*Keywords*:
Articulated Vehicle Carrying Liquid
16 degrees-of-freedom dynamic model
Lateral Load Transfer
Rollover Stability

*ABSTRACT*

In this paper, the consequences of filled volume on the transient lateral dynamic and stabilities boundaries displacement of an articulated vehicle carrying liquid is investigated. First, a sixteen-degrees-of-freedom nonlinear dynamic model of an articulated vehicle is developed. Then, the model is validated by using TruckSim software. Next, the dynamic interaction of the fluid cargo with the vehicle, by integrating a quasi-dynamic slosh model with a tractor semitrailer model is investigated. In this study, the most important dynamic reposes are considered which include yaw rate, roll angle and lateral acceleration for both the tractor and semitrailer as well as liquid center of mass lateral movement. Also, to investigate the rollover stability of the vehicle, lateral load transfer ratio is considered as an important factor. The dynamic system performance for three different filled volumes is exhibited in j-turn and lane change standard maneuvers. The simulation results revealed that by increasing the liquid volume the rollover probability rises due to the increase in roll angle and lateral load transfer, especially in lane change maneuver.

***doi****: 10.5829/idosi.ije.2015.28.11b.16*

**NOMENCLATURE**

| | | | |
|---|---|---|---|
| $CS_{t(s)}$ | Damping of the tractor's (semitrailer's) suspension | $L_{ts}$ | Distance between the semitrailer axles |
| $C_w$ | Damping of the coupling point between the tractor and the semitrailer | $m_{s(ss)}$ | Semitrailer total mass(sprung mass) |
| $D$ | Tank diameter | $m_{t(st)}$ | Tractor total mass(sprung mass) |
| $h_{ct(s)}$ | Height of the center of gravity of the tractor's (semitrailer) sprung mass to the roll axis | $R$ | The cross section radius |
| $F_{fx(fy)}$ | The longitudinal (lateral) coupling force | $R_{wi}$ | Wheel radius |
| $h_{wt(ws)}$ | Height of the fifth wheel to the roll axis of the tractor unit (semitrailer unit) | $T_i$ | The input drive torque |
| $I_{wi}$ | Wheel moment of inertia | $T_{wt(s)}$ | Track width of the trailer unit(semitrailer unit) |
| $I_{xx_{pt(ps)}}$ | Roll moment of inertia of the sprung mass of the tractor unit (semitrailer unit) | $u_{t(s)}$ | Longitudinal velocity of tractor unit(semitrailer unit) |
| $I_{xz_{pt(ps)}}$ | Roll–yaw product of inertia of the sprung mass of the tractor unit (semitrailer unit) measured about the center of gravity of the sprung mass | $v_{t(s)}$ | Lateral velocity of tractor unit(semitrailer unit) |
| $I_{zz_{t(s)}}$ | Yaw moment of the total mass of the tractor unit (semitrailer unit) measured about the center of gravity of the total vehicle mass | $z_0$ | The height of the liquid mass center in absence of roll angle and lateral acceleration of the semitrailer |
| $KS_{t(s)}$ | Roll stiffness of the tractor's (semitrailer's) suspension | $Z$ | The vertical position of liquid center of gravity |
| $K_w$ | Roll stiffness of the coupling point between the tractor and the semitrailer | $\Gamma$ | Articulation angle |
| $L$ | The length of tank | $\omega_i$ | The rotational velocity of each wheel |
| $L_{ct}$ | Distance between the tractor's center of gravity and the coupling point | $\dot{\psi}_{t(s)}$ | Yaw rate of the tractor unit (semitrailer unit) |
| $L_{ft}(L_{rt})$ | Distance between the tractor's center of gravity and the front axle (the rear axle) | $\varphi_t(s)$ | Roll angle of the tractor unit (semitrailer unit) |
| $L_{fs}(L_{rs})$ | Distance between the semitrailer's center of gravity and the coupling point (the rear axle) | $\delta$ | Steer angle |

*Corresponding Author's Email: amin_saeedi@mail.kntu.ac.ir (M. A.Saeedi)

Please cite this article as: M. A. Saeedi, R. Kazemi, S. Azadi, Liquid Sloshing Effect Analysis on Lateral Dynamics of an Articulated Vehicle Carrying Liquid for Various Filled Volumes, International Journal of Engineering (IJE), TRANSACTIONS B: Applications..Vol. 28, No. 11, (November 2015) 1671-1679

## 1. INTRODUCTION

An articulated vehicle carrying liquid includes two units, tractor and semitrailer liquid container joint by mechanical coupling. The tractor unit is located in front of the vehicle and typically involves a diesel motor and several axles which is steered by the driver. The semitrailer has wheels merely in rear and is moved by the tractor unit and is employed for material transportation. One mechanical systems in which mutual interaction exists, is articulated vehicle carrying liquid. Fluid sloshing in the tanker exerts lateral forces and moments promoting earlier rollover than other types of vehicles [1]. Rollover accidents affect strongly highway safety, especially rollover of heavy-duty tankers carrying fuels and chemicals, which might result in explosions and catastrophic chemical spills. This fact made the study of rollover stability of various vehicles, especially articulated ones carrying liquid, a major concern for many vehicle manufacturers, organizations, and researchers. Strandberg et al. [2] studied the overturning risk of heavy-duty truck-trailer combinations both analytically and experimentally. Popov et al. [3] conducted a study to obtain an optimum shape of elliptical road containers in terms of minimizing the overturning moment resulting in a vehicle rollover. Ranganathan et al. [4] analyzed the stability of partially-filled tank vehicles through computer simulations. The equations of motion for sloshing fluid within an elliptical tank were derived using Lagrange's equation assuming small amplitudes of sloshing wave. Kang et al. [5] investigated directional stability of an articulated vehicle under combined turning and braking maneuvers, a quasi-dynamic sloshing model of clean bore tank coupled with the vehicle dynamics. Roll stability analyses of partially-filled tank vehicles have further indicated that magnitude of lateral liquid sloshing under various vehicle maneuvers is strongly affected by the tank geometry, specifically the cross-section [6-9]. Kolaei et al. [10] and Shu et al. [11] employed the conformal mapping technique to obtain slosh force and overturning moment in half-filled elliptical containers equipped with vertical or horizontal side baffles under a lateral acceleration excitation. Talebi et al. [12, 13] optimized the tanker rollover threshold for the articulated vehicle carrying liquid. Azadi et al. [14] investigated the effect of tank shape on the lateral dynamic of the vehicle.

The investigation of the effect of filled volume on lateral dynamic and the most important roll dynamic responses of an articulated vehicle carrying liquid during steady state and transient maneuvers is one of the major contributions of the paper. So, this paper is organized as follows. At first, a dynamic model of an articulated vehicle is developed. Then, the dynamic model is validated by using the TruckSim software during double lane change maneuver. Next, dynamic interaction between the liquid and the vehicle, employing quasi-dynamic method is investigated. Also, Lateral load transfer ratio is studied as an important factor on the rollover stability of the articulated vehicle carrying liquid. In the fifth section of the study, the effect of liquid sloshing is examined on the dynamic responses of the vehicle in J-turn and lane change maneuvers. The simulations are carried out for three different filled volumes (low, medium and high) in various velocities. At last, the results are provided.

## 2. DYNAMIC MODELING

The sixteen degrees of freedom model reflecting the directional characteristics of the articulated vehicle is used. The articulated vehicle was modeled using two rigid bodies including the tractor with front steerable axle supplying by the driver and the semi-trailer with three axles. The considered degrees of freedom include; longitudinal and lateral velocity of the tractor, tractor yaw rate, articulation angle, tractor roll angle, trailer roll angle and wheels rotational velocity. In this model, tractor front wheels are considered steerable. As can be seen from Figure 1, five coordinate systems for the model are considered. The first three ones are: the inertial coordinate system $x_n y_n z_n$ fixed to the ground, the tractor coordinate system $x_t y_t z_t$ fixed to the tractor's center of gravity and the third is semitrailer coordinate system $x_s y_s z_s$ mounted to the semi-trailer CG. In addition, the coordinate systems, $x_s' y_s' z_s'$ and $x_t' y_t' z_t'$, are set at the center of the sprung mass of the tractor and semitrailer.

The rate of the articulation can be represented by:

$$\Gamma = \dot{\psi}_s - \dot{\psi}_t \tag{1}$$

The traction and side tire forces can be expressed in tractor and trailer coordinate systems as follows**:**

$$F_{xi} = F_{ti}\cos(\delta_i) - F_{si}\sin(\delta_i)$$
$$F_{yi} = F_{ti}\sin(\delta_i) + F_{si}\cos(\delta_i), \tag{2}$$
$$i = 1,2,\dots,10$$

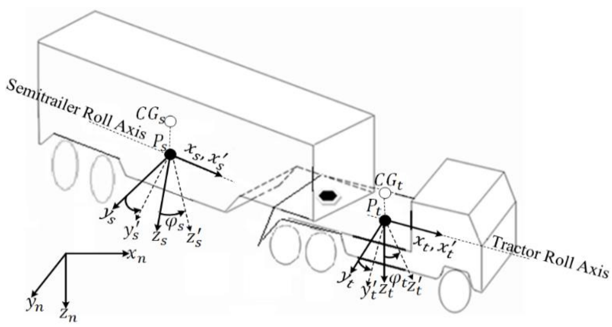


**Figure 1.** The sixteen degrees-of-freedom model.

**2. 1. Tractor Unit** Based on Figure 2, the effective external forces on system dynamics are longitudinal and lateral forces which are created at the contact locations of the tires and road and constrain forces in fifth wheel. The sum of longitudinal and lateral forces of the tractor tires is defined as:

$$F_{xtt} = F_{x1} + F_{x2} + F_{x3} + F_{x4} + F_{x5} + F_{x6}$$
$$F_{ytt} = F_{y1} + F_{y2} + F_{y3} + F_{y4} + F_{y5} + F_{y6} \quad (3)$$

Tractor yaw moment is:

$$M_{ptz} = (F_{x2} + F_{x4} + F_{x6} - F_{x1} - F_{x3} - F_{x5})\,T_w/2 + (F_{y1} + F_{y2})L_{ft} - (F_{y3} + F_{y4})L_{rt} - (F_{y5} + F_{y6})(L_{rt} + L_{tt}) \quad (4)$$

Moreover, tractor roll moment is as below:

$$M_{p_{tsx}} = m_{st} g h_t \sin(\varphi_t) - KS_t\varphi_t - CS_t\dot{\varphi}_t + KS_w(\varphi_t - \varphi_s) + CS_w(\dot{\varphi}_t - \dot{\varphi}_s) \quad (5)$$

**2. 2. Semitrailer Unit** The sum of longitudinal and lateral forces of the semitrailer tires is defined a:

$$F_{xss} = F_{x7} + F_{x8} + F_{x9} + F_{x10}$$
$$F_{yss} = F_{y7} + F_{y8} + F_{y9} + F_{y10} \quad (6)$$

Semitrailer yaw moment is:

$$M_{psz} = (F_{x8} + F_{x10} - F_{x7} - F_{x9})\,T_{ws}/2 - (F_{y7} + F_{y8})(L_{rs} - L_{ts}) - (F_{y9} + F_{y10})L_{rs} \quad (7)$$

And, tractor roll moment is:

$$M_{p_{ssx}} = m_{ss} g h_s \sin(\varphi_s) - KS_s\varphi_s - CS_s\dot{\varphi}_s - KSw(\varphi_t - \varphi_s) - CS_w(\dot{\varphi}_t - \dot{\varphi}_s) \quad (8)$$

**2. 3. The Articulated Vehicle of Equations of Motion** The governing equations of the articulated vehicle can be expressed as:

$$m_t\dot{u}_t = m_t v_t\dot{\psi}_t + m_{st} h_t\dot{\varphi}_t\dot{\psi}_t + F_{xtt} + F_{fx} \quad (9)$$

$$m_t\dot{v}_t + m_{st} h_t\ddot{\varphi}_t = -m_t u_t\dot{\psi}_t + F_{ytt} - F_{fy} \quad (10)$$

$$I_{zz_t}\ddot{\psi}_t - I_{xz_{pt}}\ddot{\varphi}_t = M_{p_{tz}} + F_{fy}L_{ct} \quad (11)$$

$$I_{xx_{pt}}\ddot{\varphi}_t - I_{xz_{pt}}\ddot{\psi}_t + m_{st}h_t\dot{v}_t = M_{p_{tsx}} - m_{st}h_t u_t\dot{\psi}_t \quad (12)$$

$$m_s\dot{u}_s = m_s v_s\dot{\psi}_s + m_{ss}h_s\dot{\varphi}_s\dot{\psi}_s + F_{xss} - F_{fx}\cos(\Gamma) + F_{fy}\sin(\Gamma) \quad (13)$$

$$m_s\dot{v}_s + m_{ss}h_s\ddot{\varphi}_s = -m_s u_s\dot{\psi}_s + F_{yss} + F_{fx}\sin(\Gamma) + F_{fy}\cos(\Gamma) \quad (14)$$

$$I_{zz_s}\ddot{\psi}_s - I_{xz_{ps}}\ddot{\varphi}_s = (F_{fx}\sin(\Gamma) + F_{fy}\cos(\Gamma))L_{ws} + M_{p_{sz}} \quad (15)$$

$$I_{xx_{ps}}\ddot{\varphi}_s - I_{xz_{ps}}\ddot{\psi}_s + m_{ss}h_s\dot{v}_s = M_{p_{ssx}} - m_{ss}h_s u_s\dot{\psi}_s \quad (16)$$

$$\dot{u}_t - \dot{u}_s\cos(\Gamma) + \dot{v}_s\sin(\Gamma) + L_{fs}\ddot{\psi}_s\sin(\Gamma) + h_{ws}\ddot{\varphi}_s\sin(\Gamma) = -\dot{u}_s\Gamma\sin(\Gamma) - \dot{\Gamma}v_s\cos(\Gamma) - L_{fs}\dot{\Gamma}\dot{\psi}_s\cos(\Gamma) - h_{ws}\dot{\Gamma}\dot{\varphi}_s\cos(\Gamma) \quad (17)$$

$$\dot{v}_t - L_{wt}\ddot{\psi}_t + h_{ct}\ddot{\varphi}_t - \dot{u}_s\sin(\Gamma) - \dot{v}_s\cos(\Gamma) - L_{fs}\ddot{\psi}_s\cos(\Gamma) - h_{ws}\ddot{\varphi}_s\sin(\Gamma) = u_s\dot{\Gamma}\cos(\Gamma) - \dot{\Gamma}v_s\sin(\Gamma) - L_{fs}\dot{\Gamma}\dot{\psi}_s\sin(\Gamma) - h_{ws}\dot{\Gamma}\dot{\varphi}_s\sin(\Gamma) \quad (18)$$

**2. 4. Tire dynamics** Here, the Duggof tire model is employed for calculation of longitudinal and lateral forces [15].

$$\lambda = \frac{\mu F_{zi}\left[1 - \varepsilon_r u_i\sqrt{S_i^2 + \tan^2(\alpha_i)}\right](1 - S_i)}{2\sqrt{C_i^2 S_i^2 + C_\alpha^2\tan^2(\alpha_i)}}$$

$$f(\lambda) = \begin{cases} \lambda(\lambda - 2) & if\,\lambda < 1 \\ 1 & if\,\lambda > 1 \end{cases} \quad (19)$$

$$F_{si} = \frac{C_\alpha\tan(\alpha_i)}{1 - S_i}f(\lambda)$$

$$F_{ti} = \frac{C_i S_i}{1 - S_i}f(\lambda)$$

**2. 5. Tire slip** In this section, longitudinal slip and side slip angle are considered [16-18].

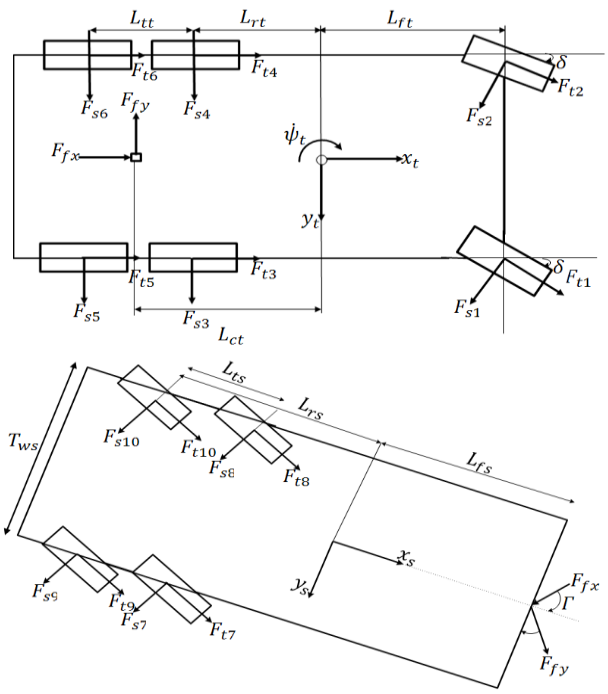


**Figure 2.** The effective external forces on tractor and semitrailer units.

### 2. 5. 1. Longitudinal Slip

$$\lambda_i = \begin{cases} (V_R \cos(\alpha) - u_i)/u_i, & (u_i \geq V_R \cos(\alpha)) \\ (V_R \cos(\alpha) - u_i)/V_R \cos(\alpha), & (V_R \cos(\alpha) > u_i) \end{cases} \quad (20)$$

### 2. 5. 2. Tire Side Slip Angle

$$\alpha_{1(2)} = \delta_f - \tan^{-1}\left(\frac{v_t + L_{ft} r_t}{u_t \overset{-}{(+)} r_t \frac{T_w}{2}}\right) \qquad \alpha_{3(4)} = -\tan^{-1}\left(\frac{v_t - r_t L_{rt}}{u_t \overset{-}{(+)} r_t \frac{T_w}{2}}\right)$$

$$\alpha_{5(6)} = -\tan^{-1}\left(\frac{v_t - r_t(L_{rt} + L_{tt})}{u_t \overset{-}{(+)} r_t \frac{T_w}{2}}\right) \qquad \alpha_{7(8)} = -\tan^{-1}\left(\frac{v_s - r_s(L_{rs} - L_{ts})}{u_s \overset{-}{(+)} r_s \frac{T_{ws}}{2}}\right)$$

$$\alpha_{9(10)} = -\tan^{-1}\left(\frac{v_s - r_s L_{rs}}{u_s \overset{-}{(+)} r_s \frac{T_{ws}}{2}}\right) \quad (21)$$

The vehicle parameters are shown in Appendix.

**2. 6. Wheel Dynamics** The following equation can be written for traction from Figure 3:

$$I_w \dot{\omega} = -R_w F_{xi} + T_i \quad (22)$$

## 3. DYNAMICS VALIDATION

In order to validate the dynamic model, TruckSim software is used [19]. So, the developed model parameters are considered the same as the ones implemented in TruckSim modeled vehicle. The simulation results of double lane change maneuver are shown in Figures 4 and 5. In this analysis, the vehicle with initial velocity of 70 $Km/h$ on a dry road with road friction coefficient of 0.7 and the above steering input is considered. As can be seen from Figure 5, the yaw rate, articulation angle and trajectory curves of the articulated vehicle matches acceptably with the one carried out TruckSim test. Moreover, although the roll angle curve shows appropriate coincidence with the TruckSim model results, some deviations between these two are observed during $t = 5 - 7\ s$.

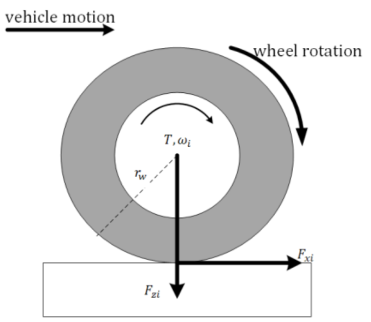


**Figure 3.** Wheel diagram [20].

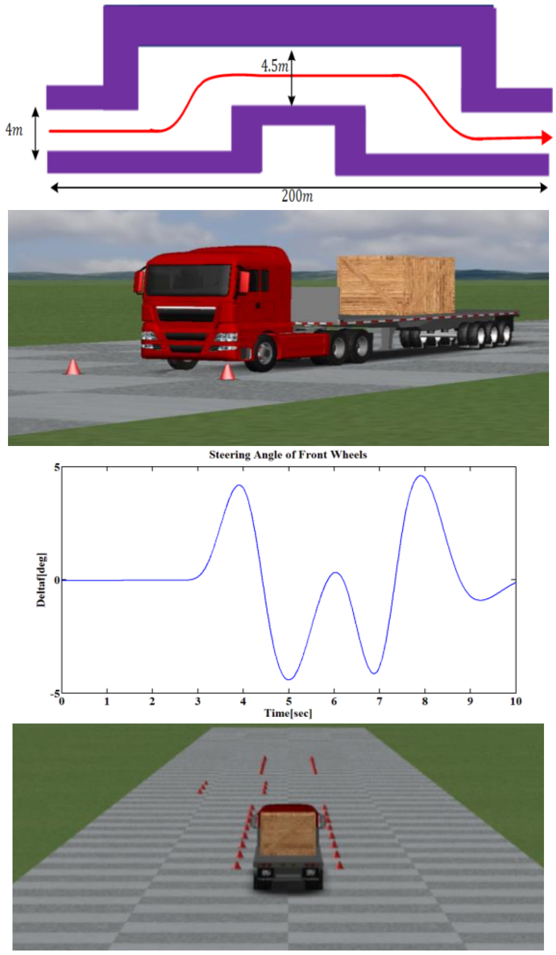


**Figure 4.** Typical 200m double lane change maneuver.

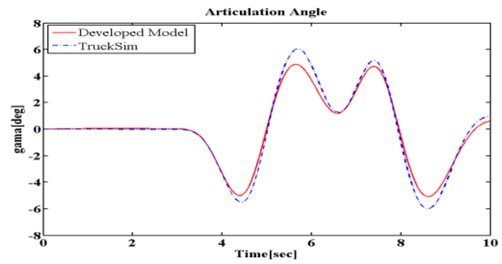


(a)

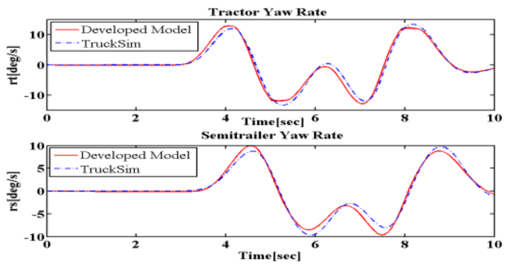


(b)

**Figure 5.** Model validation: (a) Articulation angle response, (b) tractor and semitrailer yaw rates, (c) tractor and semitrailer roll angles, (d) the vehicle trajectory.

## 4. ARTICULATED VEHICLE CARRYING LIQUID MODELING

In this study, in order to model the liquid in the tank and to study the effect of liquid load transfer on lateral dynamics of the vehicle, the quasi-dynamic method is used. In the model, the liquid due to roll angle and lateral acceleration of semitrailer moves and the liquid free surface movement leads to change of the liquid center of mass location and its moment of inertia. Also, considering roll angle and lateral acceleration of semitrailer, calculating pressure gradient and assuming invisid flow, the liquid free surface gradient is determined.

$$\tan(\emptyset) = \left(\frac{\varphi_s - a_l}{1 + a_l\varphi_s}\right) \tag{23}$$

As shown in Figure 6, for a tank of circular cross section, the vertical and lateral position of fluid center of gravity is calculated as below [21]:

$$Z = R - (R - Z_0)\cos(\emptyset)$$
$$Y = (R - Z_0)\sin(\emptyset) \tag{24}$$

where $R$ is the cross section radius and $Z_0$ the height of the fluid mass center in absence of roll angle and lateral acceleration of the semitrailer.
In addition, the liquid moment of inertia is calculated as below:

$$I_{xl} = I_{xl}^0$$
$$I_{zl} = I_{zl}^0(\cos(\emptyset))^2 \tag{25}$$

where $I_{xl}^0$ and $I_{zl}^0$ are the moments of inertia for the zero free surface gradient state.
Calculation of liquid center of mass acceleration:

$$a_l = \left(\dot{u}_s - v_s\dot{\psi}_s - h_s\dot{\varphi}_s\dot{\psi}_s - Z\dot{\varphi}_s\dot{\psi}_s - X\dot{\psi}_s^{\,2} - Y\ddot{\psi}_s\right)\hat{\imath} + \left(\dot{v}_s + u_s\dot{\psi}_s + h_s\ddot{\varphi}_s - Y\dot{\varphi}_s^{\,2} - Y\dot{\psi}_s^{\,2} + Z\ddot{\varphi}_s + X\ddot{\psi}_s\right)\hat{\jmath} + \left(Z\dot{\varphi}_s^{\,2} + X\dot{\varphi}_s\dot{\psi}_s + Y\ddot{\varphi}_s\right)\hat{k} \tag{26}$$

### 4. 1. Combined Vehicle and Liquid Dynamic Equations

Now, employing the equations of the articulated vehicle and regarding the liquid center of mass acceleration, dynamic equations of motion are evaluated as follows:

$$m_t\dot{u}_t = m_tv_t\dot{\psi}_t + m_{st}h_t\dot{\varphi}_t\dot{\psi}_t + F_{xtt} + F_{fx} \tag{27}$$

$$m_t\dot{v}_t + m_{st}h_t\ddot{\varphi}_t = -m_tu_t\dot{\psi}_t + F_{ytt} - F_{fy} \tag{28}$$

$$I_{zz_t}\ddot{\psi}_t - I_{xz_{pt}}\ddot{\varphi}_t = M_{p_{tz}} + F_{fy}L_{ct} \tag{29}$$

$$I_{xx_{pt}}\ddot{\varphi}_t - I_{xz_{pt}}\ddot{\psi}_t + m_{st}h_t\dot{v}_t = M_{p_{tsx}} - m_{st}h_tu_t\dot{\psi}_t \tag{30}$$

$$m_s\dot{u}_s + m_la_l\hat{\imath} = m_sv_s\dot{\psi}_s + m_{ss}h_s\dot{\varphi}_s\dot{\psi}_s + F_{xss} - F_{fx}\cos(\Gamma) + F_{fy}\sin(\Gamma) \tag{31}$$

$$m_s\dot{v}_s + m_{ss}h_s\ddot{\varphi}_s + m_la_l\hat{\jmath} = -m_su_s\dot{\psi}_s + F_{yss} + F_{fx}\sin(\Gamma) + F_{fy}\cos(\Gamma) + (m_s + m_l)g\sin(\varphi_s) \tag{32}$$

$$\left(I_{zz_s} + I_{zl}\right)\ddot{\psi}_s - I_{xz_{ps}}\ddot{\varphi}_s = \left(F_{fx}\sin(\Gamma) + F_{fy}\cos(\Gamma)\right)L_{ws} + M_{p_{sz}} + m_la_l\hat{\jmath}X - m_la_l\hat{\imath}Y \tag{33}$$

$$\left(I_{xx_{ps}} + I_{xl}\right)\ddot{\varphi}_s - I_{xz_{ps}}\ddot{\psi}_s + m_{ss}h_s\dot{v}_s = M_{p_{ssx}} - m_{ss}h_su_s\dot{\psi}_s + m_la_l\hat{\jmath}Z + m_la_l\hat{k}Y + m_lg(Z\sin(\varphi_s) + Y) \tag{34}$$

### 4. 2. Dynamic Model Validation

The analytical model presented in this study is validated using the actual test data given in [4]. Therefore, the dynamic model specifications are considered similar to that of the cited reference. This process is carried out for a 70 percent filled tank vehicle at velocity of 45 $km/h$ for a 15$m$ lane change maneuver as shown in Figure 7 (a).

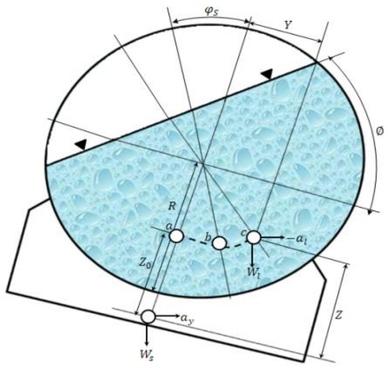

**Figure 6.** Roll plane liquid model of a partially filled circular cross section.[21]

The simulation results are compared to those established from the field tests. As can be seen from Figure 7(b), the semitrailer yaw angle is in an appropriate agreement with the mentioned reference results. Figure 7(c) shows the lateral acceleration of the semitrailer. As can be seen, the simulation results correlate very well with the field test responses.

## 5. SIMULATION RESULTS

In this section, the effect of filled volume on lateral dynamic of the articulated vehicle carrying liquid is evaluated for various speeds.

**5. 1. J-turn Maneuver** In this study, the vehicle at 60 $km/h$ initial velocity on a dry road with 0.7 friction coefficient moves and steering input is as Figure 8.

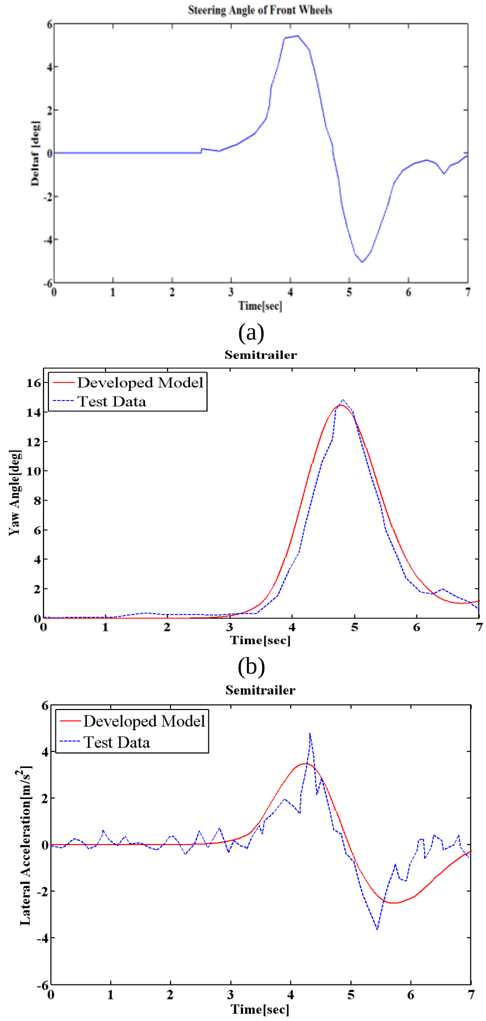

(c)

**Figure 7.** Model validation: (a) steering angle, (b) the yaw angle, (c) the lateral acceleration.

In this section, the most significant roll dynamic responses of the vehicle including yaw rate, roll angle, liquid center of mass lateral movement and lateral load transfer ratio are compared for diverse conditions. As can be seen from Figure 9, as the filled volume grows, the yaw rate increases. The amount of this increase is considerable at the third second for the semitrailer unit. According to Figure 10, as the height of the liquid rises, the roll angle for both units ascends considerably. The quantity of the increase is high at the first peak while this parameter converges to constant values for each of the volumes. Figure 11(a) demonstrates the amount of liquid mass center lateral displacement for the three filled volumes. It can be seen, an increase in the filled volume leads to a decrease in the lateral displacement. In this case, the amount of the displacement for the 30 percent filled volume is more than that for the two other conditions.

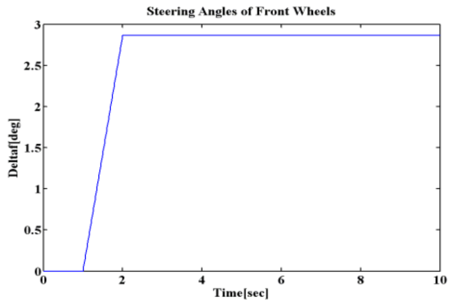


**Figure 8.** Steering angle.

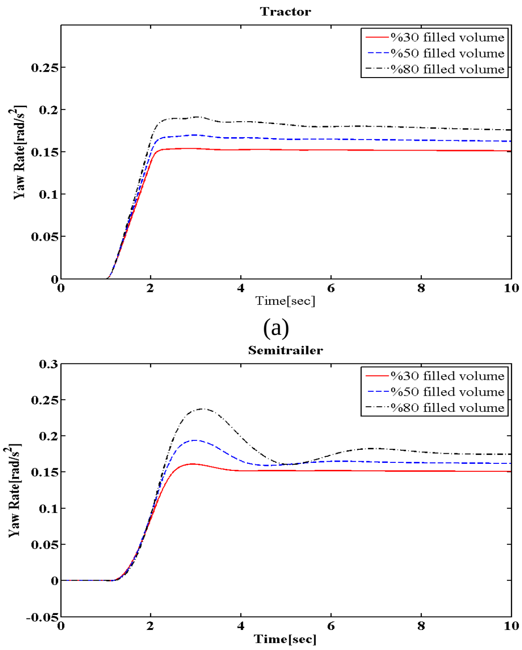

(b)

**Figure 9.** The yaw rate: (a) tractor unit, (b) semitrailer unit.

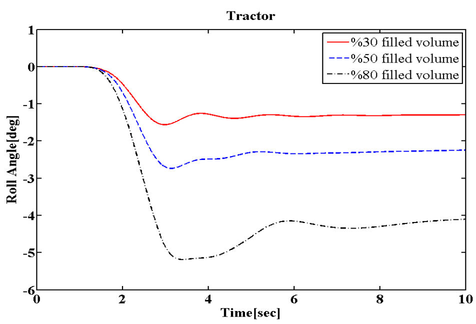

(a)

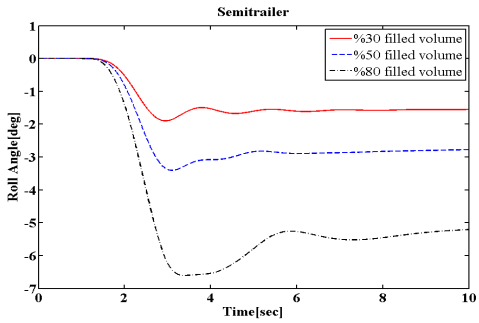


(b)

**Figure 10.** The roll angle: (a) tractor unit, (b) semitrailer unit.

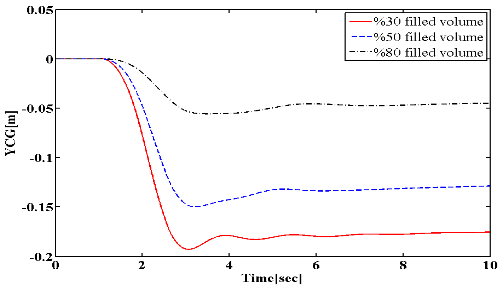


(a)

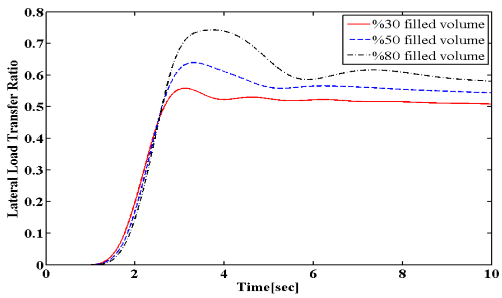


(b)

**Figure 11.** (a) Liquid lateral displacement, (b) lateral load transfer ratio.

Lateral dynamic behavior of an articulated vehicle is investigated using lateral load transfer ratio (LTR). The LTR is defined as [21]:

$$LTR = \sum_{j=1}^{N} \frac{|F_{zrj} - F_{zlj}|}{F_{zrj} + F_{zlj}} \quad (35)$$

The LTR starts from zero and becomes unity when there is no contact between the wheels and the road. Figure 11(b) also demonstrates that at the first peak a considerable increase is observed for 80 percent filled volume which is due to the dynamic interaction between the vehicle and the liquid cargo.

**5. 2. Lane Change Maneuver** In this maneuver, the vehicles run on a level icy road with a friction coefficient of 0.4 at the constant speed of 90 $km/h$ and the steering angle input shown in Figure 12. According to Figure 13, the roll angle increases for both units when the volume goes up. The amount of this increase for the second part of the maneuver is more in comparison with roll angle in first peak.

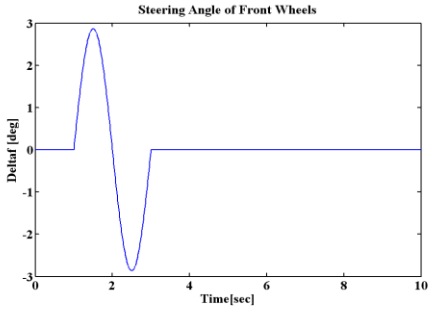


**Figure 12.** Steering angle.

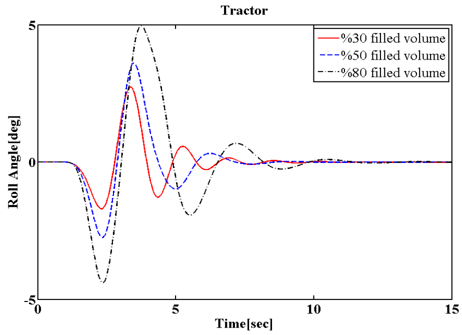


(a)

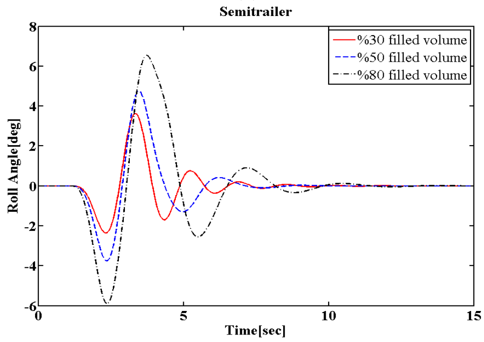


(b)

**Figure 13.** The roll angle: (a) tractor unit, (b) semitrailer unit.

Moreover, For the 30 and 50 percent filled volumes, the roll angle reaches zero after 7 seconds while this portion is 11 seconds for the 80 percent filled case.

## 7. CONCLUSION

In this paper, the effect of liquid sloshing is investigated on the lateral dynamic of an articulated vehicle carrying liquid in transient and steady state maneuvers. At first, a thorough nonlinear model for the articulated vehicle is developed. Then using quasi-dynamic method for the carried liquid modeling, the dynamic interactions between the vehicle and the liquid is studied.

Then, the dynamic system performance is compared in J-turn and transient maneuvers for 3 liquid volumes for which the following conclusions are derived.

- The vehicle roll dynamic responses are intensely subjected to the liquid sloshing.
- As the liquid level ascends, the roll angle increases.
- For the least filled volume, the liquid center of mass movement boosts.
- The filled volume increment leads to minor effects on the yaw rate and lateral acceleration of the tractor unit.
- The rollover stability is greatly affected by the filled volume. Increasing the liquid volume, increases the lateral load transfer ratio. This increase is much more recognizable for the second peak which is due to the interaction between the liquid and the vehicle.

## 8. REFERENCES


1. Ervin, R., Barnes, M. and Wolfe, A., *Liquid cargo shifting and the stability of cargo tank trucks. Volume 2. Final technical report*. (1985).
2. Strandberg, L., *Lateral stability of road tankers. Volume 1, main report. Volume 2, appendices*. (1978).
3. Popov, G., Sankar, S. and Sankar, T., "Shape optimization of elliptical road containers due to liquid load in steady-state turning", ***Vehicle System Dynamics***, Vol. 25, No. 3, (1996), 203-221.
4. Ranganathan, R., "Stability analysis and directional response characteristics of heavy vehicles carrying liquid cargo", Concordia University, (1990),
5. Kang, X., Rakheja, S. and Stiharu, I., "Cargo load shift and its influence on tank vehicle dynamics under braking and turning", ***International Journal of Heavy Vehicle Systems***, Vol. 9, No. 3, (2002), 173-203.
6. Winkler, C.B. and Ervin, R., "Rollover of heavy commercial vehicles, Society of Automotive Engineers, (2000).
7. Liu, Z. and Huang, Y., "A new method for large amplitude sloshing problems", ***Journal of Sound and Vibration***, Vol. 175, No. 2, (1994), 185-195.
8. Ibrahim, R.A., Pilipchuk, V. and Ikeda, T., "Recent advances in liquid sloshing dynamics", ***Applied Mechanics Reviews***, Vol. 54, No. 2, (2001), 133-199.
9. Kazemi, R. and Saeedi, M.A., "A new robust active roll control system for improving roll stability of an articulated vehicle carrying liquid", ***Moddares Mechanical Engineering***, Vol. 15, No. 6, (2015), 353-364.
10. Kolaei, A., Rakheja, S. and Richard, M.J., "Three-dimensional dynamic liquid slosh in partially-filled horizontal tanks subject to simultaneous longitudinal and lateral excitations", ***European Journal of Mechanics-B/Fluids***, Vol. 53, (2015), 251-263.
11. Shu-en, Z. and Ling-he, Z., "Dynamic simulation of liquid sloshing characteristics for tank trucks in lateral movement", ***Applied Mathematics & Mechanics (1000-0887)***, Vol. 35, No. 11, (2014) 135-147.
12. Talebitooti, R., Shojaeefard, M. and Yarmohammadisatri, S., "Shape design optimization of cylindrical tank using b-spline curves", ***Computers & Fluids***, Vol. 109, (2015), 100-112.
13. Shojaeefard, M., Talebitooti, R., Satri, S.Y. and Amiryoon, M.H., "Investigation on natural frequency of an optimized elliptical container using real-coded genetic algorithm", ***Latin American Journal of Solids and Structures***, Vol. 11, No. 1, (2014), 113-129.
14. Azadi, S., Jafari, A. and Samadian, M., "Effect of tank shape on roll dynamic response of an articulated vehicle carrying liquids", ***International Journal of Heavy Vehicle Systems***, Vol. 21, No. 3, (2014), 221-240.
15. Dugoff, H., Fancher, P. and Segel, L., *An analysis of tire traction properties and their influence on vehicle dynamic performance*., SAE Technical Paper. (1970)
16. Mirzaei, A., Moallem, M. and Mirzaeian, B., "Designing a genetic-fuzzy anti-lock brake system controller", in Intelligent Control,. Proceedings of the IEEE International Symposium on, Mediterrean Conference on Control and Automation, IEEE., (2005), 1246-1250.
17. Moghadam-Fard, H. and Samadi, F., "Active suspension system control using adaptive neuro fuzzy (ANFIS) controller", ***International Journal of Engineering-Transactions C: Aspects***, Vol. 28, No. 3, (2014), 396.
18. Saeedi, M., Kazemi, R., Rafat, M. and Pasdar, A., "Real world modeling and nonlinear control of an electrohydraulic driven clutch", ***International Journal of Automotive Engineering***, Vol. 2, No. 2, (2012), 107-116.
19. Mechanical Simulation Corporation (MSC), T.R.M., " in., (1999).
20. Saeedi, M. and Kazemi, R., "Stability of three-wheeled vehicles with and without control system", ***International Journal of Automotive Engineering***, Vol. 3, No. 1, (2013), 343-355.
21. Kang, X., "Optimal tank design and directional dynamic analysis of liquid cargo vehicles under steering and braking", Citeseer, (2001),


## APPENDIX

**TABLE 1.** Vehicle parameters

| Parameter | Value | Unit |
|---|---|---|
| $CS_{tf(tr)}$ | 4.05(6.88) | KN. m. s/rad |
| $CS_s$ | 23.9 | KN. m. s/rad |
| $C_w$ | 700 | KN. m. s/rad |
| $D$ | 2.03 | m |
| $h_{ct(s)}$ | 0.438(1.8) | m |
| $h_{wt(ws)}$ | 0.63(1) | m |
| $I_{wi}$ | 11.63 | Kg. m$^2$ |
| $I_{xx_{pt(ps)}}$ | 3335(120024) | Kg. m$^2$ |
| $I_{xz_{pt(ps)}}$ | 602(5756) | Kg. m$^2$ |
| $I_{zz_{t(s)}}$ | 20679(238898) | Kg. m$^2$ |
| $KS_{tf(tr)}$ | 380(684) | KN. m/rad |

| | | |
|---|---|---|
| $KS_s$ | 800 | KN. m/rad |
| $K_w$ | 30000 | KN. m/rad |
| $L$ | 10 | m |
| $L_{ct}$ | 1.959 | m |
| $L_{fs}(L_{rs})$ | 5.653(2.047) | m |
| $L_{ft}(L_{rt})$ | 1.115(2.583) | m |
| $L_{tt}(L_{ts})$ | 1.31 | m |
| $m_{s(ss)}$ | 6525(4819) | Kg |
| $m_{t(st)}$ | 33221(30821) | Kg |
| $R_{wi}$ | 0.4 | m |
| $W_{t(s)}$ | 2.04(2) | m |
| $\rho$ | 1000 | $Kg/m^3$ |

# Liquid Sloshing Effect Analysis on Lateral Dynamics of an Articulated Vehicle Carrying Liquid for Various Filled Volumes

M. A. Saeedi, R. Kazemi, S. Azadi

*Department of Mechanical Engineering, K. N. Toosi University of Technology, Tehran, Iran.*

*PAPER INFO*

*Paper history:*
Received 15 July 2015
Received in revised form 12 November 2015
Accepted 19 November 2015

*Keywords*:
Articulated Vehicle Carrying Liquid
16 degrees-of-freedom dynamic model
Lateral Load Transfer
Rollover Stability

**چکیده**

در این مقاله تاثیر حجم پرشدگی، بر دینامیگ گذرا و جابه‌جایی مرزهای پایداری خودروی مفصلی حامل سیال بررسی شده است. برای این منظور، ابتدا یک مدل دینامیکی با شانزده درجه آزادی از خودروی مفصلی تدوین شد. سپس، مدل با استفاده از نرم‌افزار تراک سیم صحه‌گذاری گردید. اندرکنش دینامیکی بین بار سیال و خودرو با ترکیب روش شبه دینامیکی برای مدل‌سازی سیال درون مخزن و به کارگیری یک مدل دینامیکی غیرخطی شانزده درجه آزادی خودروی مفصلی بررسی شده است. در این بررسی مهم‌ترین پاسخ‌های دینامیکی شامل سرعت زاویه‌ای چرخشی، زاویه‌ی رول، شتاب جانبی واحد کشنده و واحد شبه‌تریلر و جابه‌جایی مرکز جرم سیال در نظر گرفته شدند. سپس، به منظور بررسی پایداری واژگونی خودروی مفصلی حامل سیال، نسبت انتقال بار جانبی به عنوان یک عامل مهم بررسی شد. عملکرد سیستم دینامیکی برای سه حجم پرشدگی مختلف در مانورهای استاندارد گردش حالت مانا و تعویض خط نشان داده شده است. نتایج شبیه‌سازی بر افزایش احتمال وقوع واژگونی با افزایش حجم سیال درون مخزن، به دلیل افزایش زاویه‌ی رول و انتقال بار جانبی، مخصوصاً در مانور تعویض خط تاکید می‌نمایند.

***doi***:*10.5829/idosi.ije.2015.28.11b.16*